ELSEVIER

Contents lists available at ScienceDirect

Estuarine, Coastal and Shelf Science

journal homepage: www.elsevier.com/locate/ecss





Assessment of short-term spatio-temporal variability in the structure of mesozooplankton communities integrating microscopy and multigene high-throughput sequencing

Lidia Yebra ^{a,*}, Candela García-Gómez ^a, Nerea Valcárcel-Pérez ^a, Alma Hernández de Rojas ^b, Leocadio Blanco-Bercial ^c, M. Carmen Castro ^b, Francisco Gómez-Jakobsen ^a, Jesús M. Mercado ^a

- ^a Centro Oceanográfico de Málaga (IEO, CSIC), 29640, Fuengirola, Spain
- ^b Centro Oceanográfico de Gijón (IEO, CSIC), 33212, Gijón, Spain
- ^c Bermuda Institute of Ocean Sciences, GE 01, St. George's, Bermuda

ARTICLE INFO

Keywords: 18S rRNA V9 Integrative taxonomy Metabarcoding Microscopy mtDNA COI SW Mediterranean Zooplankton biodiversity

ABSTRACT

Variability in composition and structure of the mesozooplankton communities in the Bay of Malaga (SW Mediterranean) were characterized during a 26 h cycle using an integrative taxonomic approach. We combined microscopic identification of organisms, with metabarcoding for the genes of the mitochondrial DNA COI and the V9 hypervariable region of the ribosomal RNA 18S. Richness and diversity obtained by microscopy were higher than those measured with COI, as COI did not detect some phyla. COI however allowed for the identification to species level of several taxa that were left at higher taxonomic rank under the microscope. 18S detected a wider range of taxa than COI and microscopy, although with lower taxonomic resolution. Differences between coastal-night and shelf-day zooplankton communities structure were detected by both microscopy and metabarcoding. The combination of these two approaches increased the known copepod species in the SW Mediterranean Sea by 9%. An integrative approach combining morphology and COI metabarcoding is proposed to further facilitate mesozooplankton biodiversity studies.

1. Introduction

Mesozooplankton are the main predator of microplankton, and prey for fishes, therefore playing a key role in marine productivity and biogeochemical fluxes (Steinberg and Landry, 2017). In addition, their short life cycle make them sensitive to environmental changes (Richardson, 2008; Bedford et al., 2020), being important indicators of the environmental state of the oceans. There is a growing need for high-resolution monitoring of marine biodiversity in order to provide detailed information on the changes that the increasing anthropogenic-induced pressures are producing on the marine environment, at local to global scales (Coll et al., 2010). However, characterization and forecast of spatial and temporal variability patterns in marine zooplankton assemblages is challenging. Traditional monitoring of zooplankton communities is achieved mainly through microscopy, with the inherent caveats of high expertise required, time-consuming analyses, cryptic species misidentification and/or lack of specificity for some young and larval stages (Cornils and Held, 2014). Still, this

knowledge is key to understand the marine ecosystems, and to advise on sustainable management of the services and resources they provide. In the past two decades, important advances in molecular tools have been achieved to improve zooplankton identification, reducing the costs and uncertainties compared to the morphological analyses (Lindeque et al., 2013; Bucklin et al., 2016). These methods also give new insights on the composition and diversity of marine coastal communities (Abad et al., 2017; Hirai et al., 2017; Stefanni et al., 2018; García-Gómez et al., 2020) as well as their trophic relationships (Leray et al., 2013; Albaina et al., 2016; Yebra et al., 2019). However, there is no standard molecular protocol suitable to detect all zooplankton taxa, nor true estimates of total abundances or biomass, only compositional data, and different new tools and approaches provide different types of information (Corell and Rodríguez-Ezpeleta, 2014). In recent years, many studies have attempted to establish relationships between morphology- and DNA-based data describing zooplankton communities' composition in the field. Their main aim was to assess the suitability of metabarcoding as substitute or as a complementary tool to microscopy to be incorporated in long-term

E-mail address: lidia.yebra@ieo.csic.es (L. Yebra).

^{*} Corresponding author.

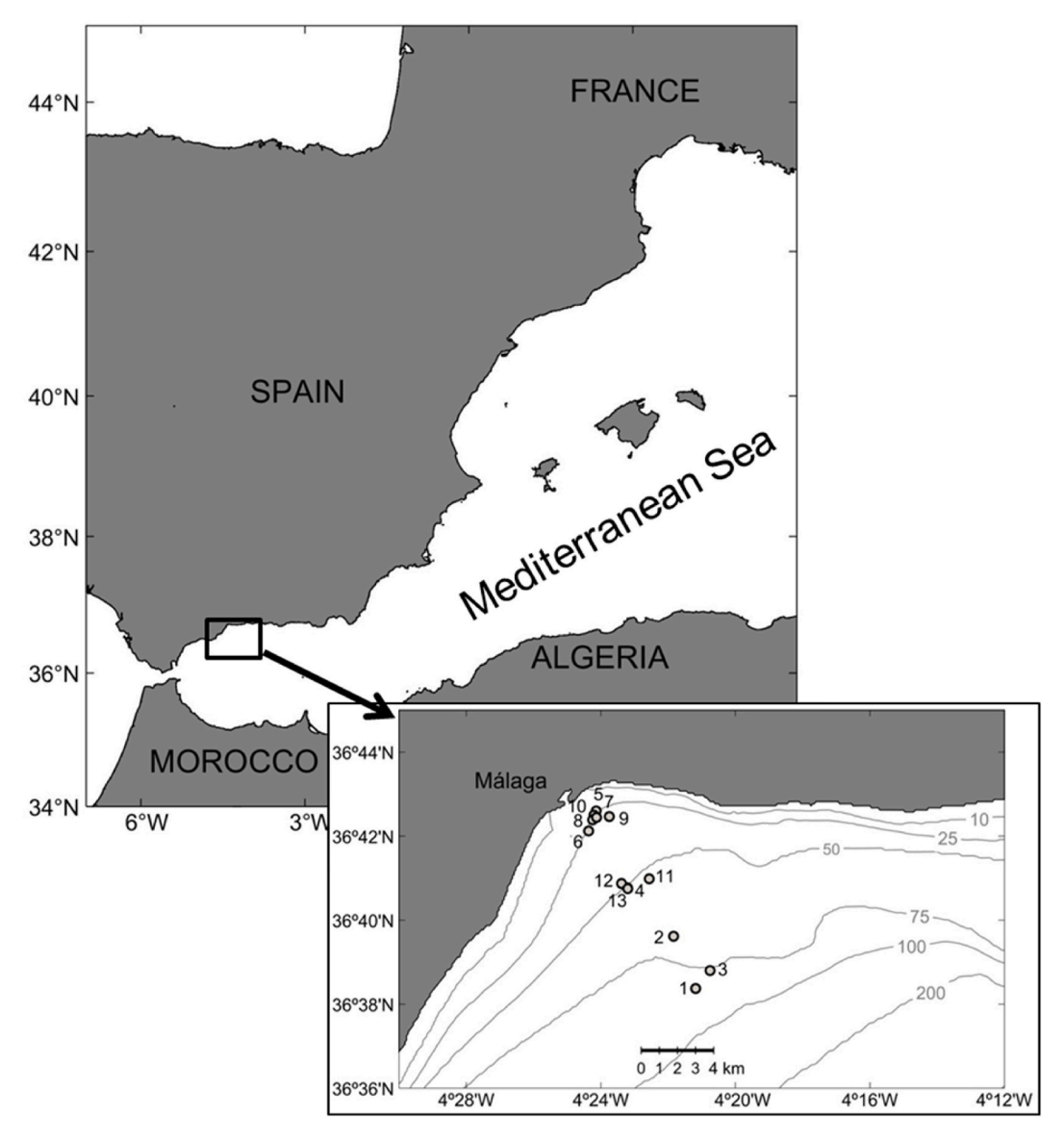


Fig. 1. Sampling stations location in the W Mediterranean Sea.

monitoring programs. Several molecular markers have been applied to characterize zooplankton community structure and diversity with different results (e.g. Questel et al., 2021; Schroeder et al., 2021). Among them, 18S ribosomal RNA hypervariable region V9 (hereafter 18S) and mitochondrial DNA cytochrome oxidase I (hereafter COI) genes seem rather good candidates to be incorporated into time series studies (Amaral-Zettler et al., 2009; Blanco-Bercial, 2020). However, to date, microscopic identification is still much needed to validate molecular procedures, or to obtain true abundances.

The Bay of Malaga, in the Western Mediterranean Sea, is a hotspot of planktonic biodiversity and productivity (Mercado et al., 2007; Yebra et al., 2017, 2018). The system is influenced by high mesoscale dynamics driven by the entrance of Atlantic waters into the Mediterranean through the Strait of Gibraltar, as well as recurrent upwelling events driven by westerly winds (Sarhan et al., 2000, Gómez-Jakobsen et al., 2019). The bay also harbors the most important nursery site in the Mediterranean Sea for the zooplanktivorous forage fishes Sardina pilchardus and Engraulis encrasicolus (García et al., 1988; Giannoulaki et al., 2013). Given the ongoing climate change and the anthropogenic pressures to which the region is being subjected (Micheli et al., 2013), optimization of zooplankton communities monitoring in the region is crucial, as changes in their composition and structure could have

important socio-economic impacts for the Western Mediterranean region (Yebra et al., 2019, 2020); such as decline in artisanal fisheries stocks or changes in environmental status affecting its attractiveness for tourism.

Our study area is a complex region with intensive mesoscale hydrodynamics through the year. Therefore, the ideal molecular marker would need to identify the components of the zooplankton community but also to detect changes in their structure within reduced space and time scales. In order to explore the adequacy of molecular tools to assess field mesozooplankton community composition and structure, as well as their short-term spatio-temporal variability, we applied an integrative taxonomic approach, combining microscope counts with high-throughput sequencing of the COI and 18S genes, to mesozooplankton samples collected every 2 h during a 26-h cycle within the Bay of Malaga.

2. Material and methods

2.1. Sampling

Sampling took place on board R/V Francisco de Paula Navarro, on 8-9th November 2014, within the Bay of Málaga, North Alboran Sea (SW

Table 1 Stations location, bottom depth (m), sampling time (GMT+1), identification methods applied (M: microscopy, COI: mtCOI, 18S: 18S V9), mean (\pm SD) water column temperature (T, °C), salinity (S), Chl a (ug·L $^{-1}$), diatoms (cells·mL $^{-1}$), dinoflagellates (cells·mL $^{-1}$), flagellates (cells·mL $^{-1}$), and ciliates (cells·mL $^{-1}$) concentration, within the coast and shelf zones. Bold font indicates night period.

Station	Latitude	Longitude	Bottom depth	Sampling time	Method applied	T	S	Chl a	Diatoms	Dinoflagellates	Flagellates	Ciliates
Coast												
5	36.710	-4.402	20.0	20:26	COI	15.15	37.45	0.54	8.24	4.55	83.57	5.4
6	36.702	-4.406	17.7	22:34	M, COI, 18S	15.90	37.17	0.49	18.8	3.26	172.5	6.94
7	36.708	-4.403	20.8	0:34	COI	15.51	37.30	0.57	14.83	11.04	78.125	12.81
8	36.706	-4.404	22.0	2:44	M, COI	15.61	37.25	0.80	41.91	10.55	93.21	3.33
9	36.708	-4.396	21.8	4:39	COI	15.83	37.16	0.94	20.83	5.9	75.94	8.63
10	36.707	-4.402	22.0	6:40	M, COI, 18S	15.58	37.26	0.85	16.93	15.56	240	10
Mean \pm			20.7 \pm			15.60 \pm	$37.26~\pm$	$0.70 \pm$	20.3 \pm	8.5 ± 4.7	123.9 \pm	7.9 \pm
SD			1.7			0.27	0.11	0.19	11.5		67.5	3.4
Shelf								<u> </u>				· <u></u>
1	36.639	-4.353	80.0	12:38	COI	14.39	37.72	0.38	30.31	4.69	93.22	7.81
2	36.660	-4.364	63.9	14:51	M, COI, 18S	14.67	37.64	0.80	17.55	5.45	60	7.5
3	36.647	-4.346	73.4	17:07	COI	14.72	37.55	0.90	24.13	9.21	86.79	18.8
4	36.679	-4.387	46.9	18:36	M, COI	15.35	37.35	0.97	39.03	14.64	66.8	5.49
11	36.683	-4.376	48.0	9:08	COI	15.59	37.16	1.09	48.28	10.29	358.59	20.06
12	36.681	-4.390	45.9	10:58	M, COI	14.86	37.56	0.58	13.17	8.04	159.87	11.61
13	36.679	-4.387	47.0	12:49	M, COI, 18S	14.59	37.71	0.52	16.08	5.52	298.125	7.27
Mean \pm			57.9 \pm			14.88 \pm	37.53 \pm	$0.75~\pm$	26.9 \pm	8.3 ± 3.5	160.5 \pm	11.2 \pm
SD			14.4			0.43	0.21	0.26	13.0		120.4	5.9

Mediterranean). Thirteen stations were sampled during a 26 h cycle, in which mesozooplankton was collected every 2 h with a double-WP2 net (200 μm mesh) by means of vertical hauls, from 3 m above the bottom to the surface (Fig. 1, Table 1). Once on board, zooplankton were carefully rinsed, and preserved in 96% undenatured ethanol. One cod-end was kept for morphological analyses, while the second cod-end was used for molecular assays.

A CTD SBE-25 was used to obtain vertical profiles of temperature and salinity at each sampling site. Seawater at the surface and the subsurface chl a fluorescence maximum depth was collected with Niskin bottles. For chlorophyll a (Chl a) concentration measurements, 1 L of seawater was filtered through a Whatman GF/F filter and immediately frozen at $-20~{\rm ^{\circ}C}$. In the laboratory, Chl a concentration (µg L $^{-1}$) was determined by spectrophotometry after extracting the pigments in 90% acetone overnight at 4 $^{\circ}$ C. Averaged Chl a concentrations were calculated for each station. Additional water samples were fixed in dark glass bottles with Lugol's solution (2% f.c.) for analyses of nano- and microplankton abundance. Once in the laboratory, 100 mL of the fixed samples sedimented in a composite chamber for 48 h following the technique developed by Utermöhl (1958). Abundances of diatoms, dinoflagellates, flagellates and ciliates were determined with a Nikon Eclipse TS100 inverted microscope.

2.2. Microscopy

Zooplankton abundance and taxonomic composition at seven stations (Table 1) were determined using a stereomicroscope (Leica M165C). Taxonomic identification was made according to Rose (1933), Trégouboff and Rose (1957) and Razouls et al. (2021). Copepod identification to species level was not always feasible, due to the presence of cryptic species in the study area.

2.3. 18S metabarcoding

Total DNA was extracted from a 5% aliquot of four ethanol-preserved samples (Table 1) at the Genomic Services, Fundación Parque Científico de Madrid (Spain), following the procedure provided with DNeasy Blood and Tissue Kit (Qiagen), with some modifications. The buffer selected

for the first step was PBS (600 $\mu L)$ and the incubation with the proteinase was prolonged to 15 min. Purified DNAs were quantified by Quant-iTTM PicoGreen® dsDNA kit (Invitrogen). For generation of 18S libraries, 3 ng of input DNA was used in a first PCR of 20 cycles with Q5® Hot Start High-Fidelity DNA Polymerase (New England Biolabs) in the presence of 200 nM primers for 18S amplification (1389F-CS1 and 1510R-CS2, Amaral-Zettler et al., 2009). A second PCR of 12 cycles was performed on the PCR product with Q5® Hot Start High-Fidelity DNA Polymerase (New England Biolabs) in the presence of 400 nM illumina-specific primers (5'-AATGATACGGCGACCACCGAGATCTACACTGACGACATGG TTCTACA-3' and 5'-CAAGCAGAAGACGGCATACGAGAT-[BC]-TACGG TAGCAGAGACTTGGTCT-3') of the Access Array Barcode Library for Illumina Sequencers (Fluidigm). The obtained amplicons were validated and quantified by Agilent 2100 Bioanalyzer using a DNA7500 LabChip kit. An equimolar pool was purified by agarose gel electrophoresis and titrated by quantitative PCR using the Kapa-SYBR FAST qPCR kit for Light Cycler 480 and a reference standard for quantification. Sequencing was performed using the Illumina MiSeq (2x200 bp paired-end). Demultiplexed samples were analyzed in MOTHUR ver. 1.43.0. (Schloss et al., 2009). The fully annotated script is available at https://gi thub.com/blancobercial/Malaga. Contigs were made allowing for trimming outside the overlapping region (therefore only reads giving full length in both directions were retained in a later cleaning step). Positions that reported different bases in each strand were left as ambiguous if the difference in quality was <10, and bases that were compared to a gap in the other strand were eliminated if the quality score was below 30. After pairing, all reads containing any ambiguity or shorter than 115 bp were removed. Sequences were aligned against the V9 region of the SILVA 128 release database (Quast et al., 2013). Sequences were trimmed to the length of the V9 region, and only those showing completeness (starting in the first base and ending in the last base of the alignment) were kept, avoiding artificial operational taxonomic units (OTUs)/amplicon sequence variants (ASVs) due to unfinished amplifications. Chimeras were removed using UCHIME (Edgar et al., 2011) as implemented in MOTHUR, and unique sequences selected. PCR errors were removed using a precluster step using UNOISE (Edgar, 2016) as implemented in MOTHUR, with a single base difference threshold. 100% OTUs (ASVs) were taxonomically assigned to a

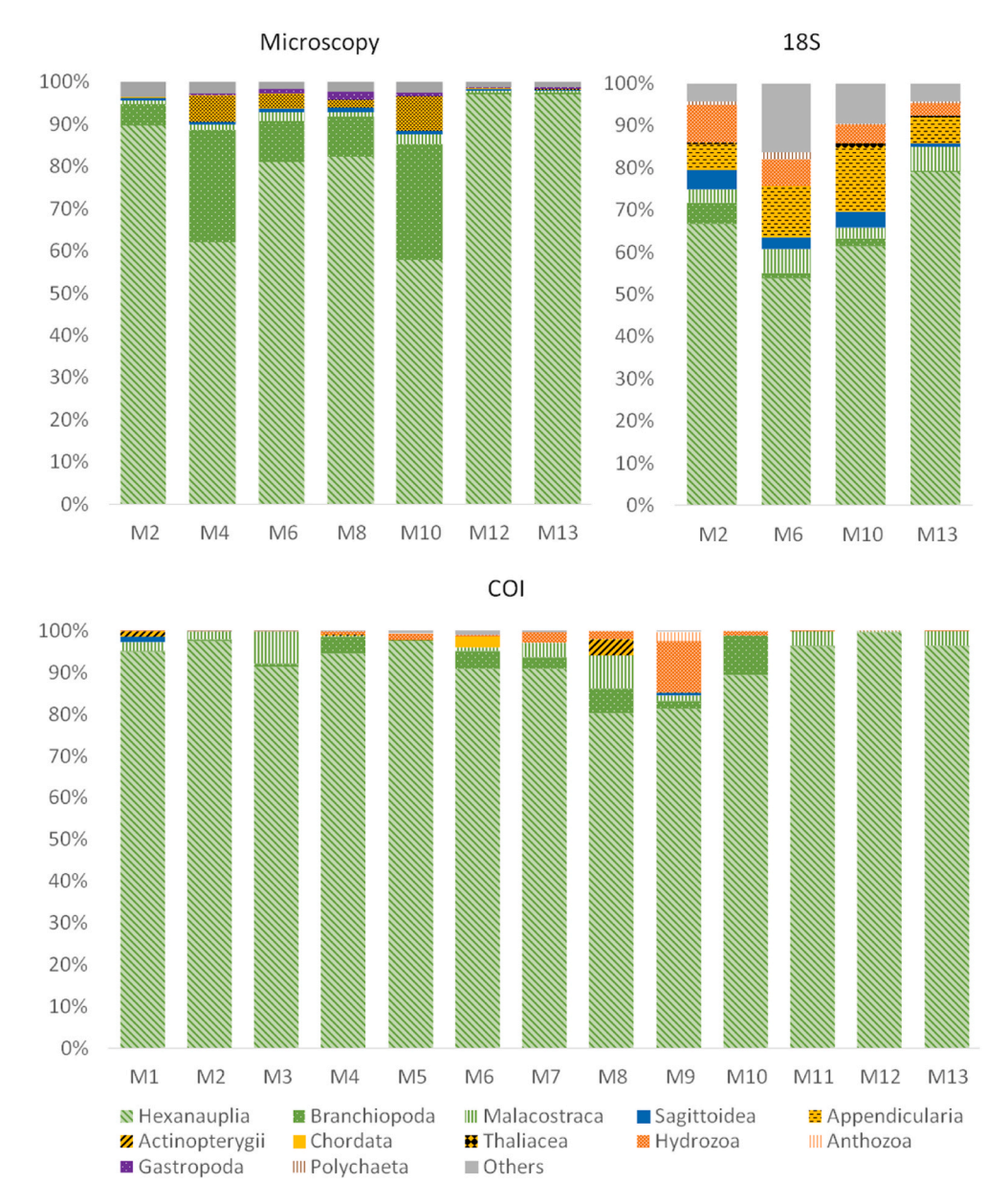


Fig. 2. Field mesozooplankton relative abundances grouped by phyla (colors) and classes (patterns) identified by A) microscopy, B) 18S, and C) COI, at each station. Taxa with abundance <1%, or not identified to phylum level, were grouped in Others. (For interpretation of the references to color in this figure legend, the reader is referred to the Web version of this article.)

database developed from the complete SILVA 128 nr release database for SSU created as in Blanco-Bercial (2020). Based on this classification, only metazoan data were selected for all downstream analyses. For identification of taxa (OTUs) flagged by ecological analyses (see below), each of the OTU were BLASTed against the GenBank and results individually analyzed, to take into account the limits of taxonomic assignment of the V9 region and the existing references.

Before further analyses, samples were standardized to the minimum number of reads per sample, and global singletons removed. OTUs with $\geq 90\%$ identity to the reference database barcode were considered assignable.

2.4. COI metabarcoding

Total DNA was extracted from thirteen ethanol-preserved samples using DNeasy Blood & Tissue kit (Qiagen), from 5% of each zooplankton sample (Table 1), as in Yebra et al. (2019). DNA pools were stored at $-20~^{\circ}$ C until their assay.

To generate COI barcodes we used the mtCOI amplification primers COIint1f (Leray et al., 2013) and dgHCOr (Meyer, 2003). As the samples were collected within the frame of a wider study on pelagic trophodynamics (Yebra et al., 2019), a fish blocking primer was added in a ratio 1:2.5 (N. Rodríguez-Ezpeleta et al., AZTI, Sukarrieta, Spain, pers. comm.). DNA amplification were performed in 20 μ L reactions with 0.4 μ L of forward and reverse primers (10 μ M) and 1 μ L of blocking primer (10 μ M), 10 μ L of 2xPhusion High-Fidelity Master Mix (Thermo Fisher Scientific) and 20 ng of DNA. PCR thermal cycling conditions were: 98 °C for 3 min, 27 cycles of 15 s at 98 °C, 30 s at 46 °C and 45 s at 72 °C; and a final extension step of 30 s at 72 °C.

Sequencing of the COI was carried out at SGIKER facilities at the University of the Basque Country (UPV/EHU). Briefly, libraries were constructed using Nextera XT index kit (Illumina) according to the manufacturer's instructions. Sequencing was performed using the Illumina MiSeq (2x300 bp paired-end).

The MOTHUR pipeline was adapted to take into account that COI region amplified exceeded the 300 bp length maximum for Illumina.

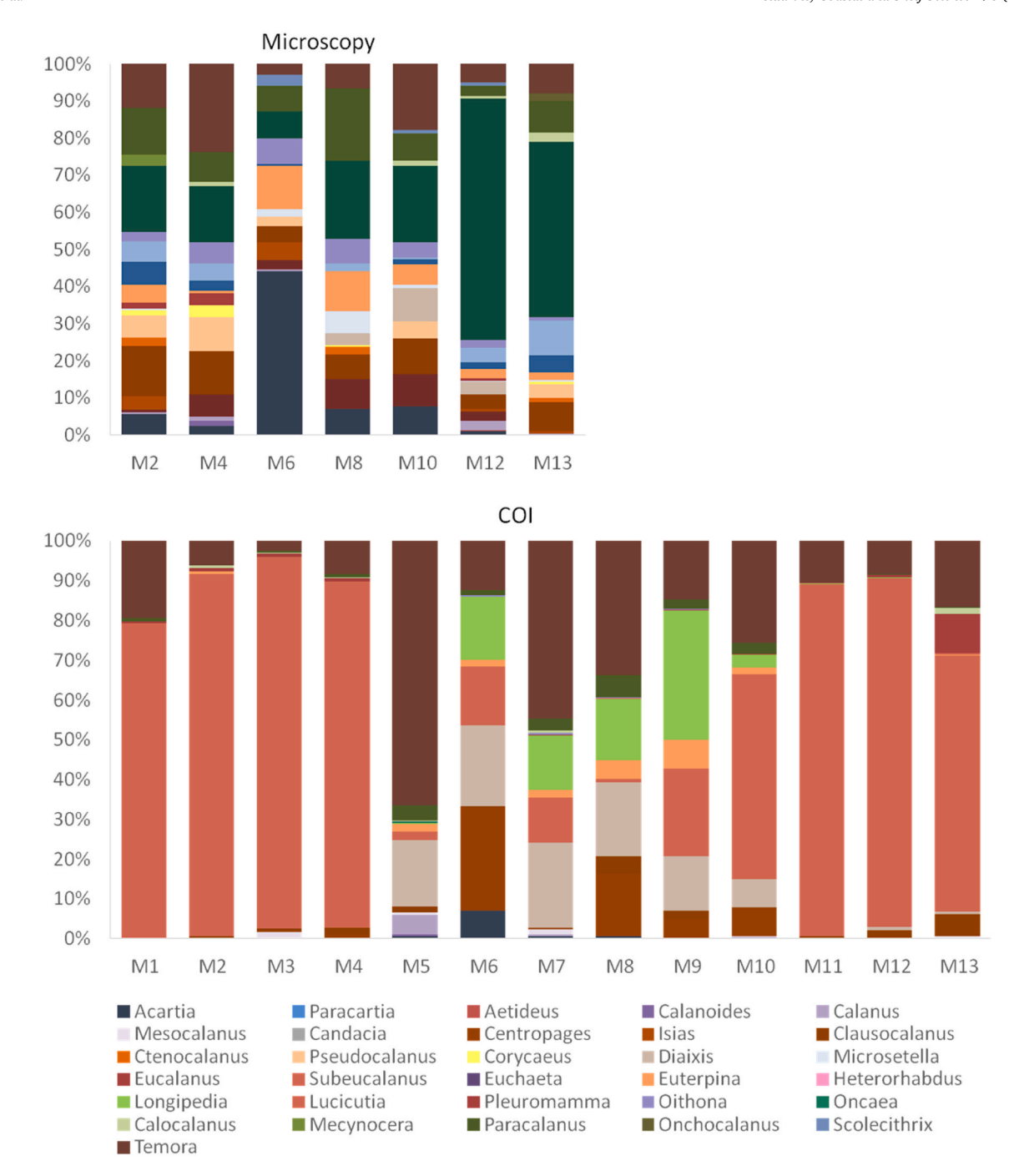


Fig. 3. Field copepod relative abundances grouped by genus identified by A) microscopy and B) COI, at each station.

Differences included: contigs were assembled with a minimum overlap of 25 bp; the non-overlapping regions were not trimmed; minimum length was 250 bp; no alignment step was done. Classification of the 100% OTUs/ASVs obtained after MOTHUR pipeline analysis was done using BLAST (Altschul et al., 1990), with GenBank (nt) as reference database barcode (accessed June 11, 2020). All other steps were those as described for the 18S V9. All scripts are available at https://github.com/blancobercial/Malaga. After classification, OTUs with \geq 90% identity were considered assignable to the order or class level. All OTUs with <90% identity to the database were flagged as unassigned. ASVs sharing the same Genbank species ID, and with >97% similarity between them, were assumed to be haplotypes of the same species and pooled together as OTUs for final analyses.

2.5. Statistical analyses

Metabarcoding samples were standardized to 10,000 reads per sample to account for samples with low number of reads, being the smallest number of raw reads 13,586 for COI and 79,445 for 18S. Only samples taxonomically assigned were retained for subsequent analyses. Taxa richness and diversity indices of data obtained with each of the three identification approaches were calculated in Primer 7 (Clarke and Gorley, 2015) on the standardized dataset. Pearson correlations were performed with Statistica 7 to assess the relationships between the results obtained by each of the three methods, after square-root transformation of mesozooplankton data with Primer. Community ecology analyses were run in R using the package Vegan (Oksanen et al. 2019). A community dissimilarity data matrix based on relative frequencies of

Table 2
Comparison between metabarcoding (reads %) and microscopy (counts %) relative abundances in the coast and shelf zones. Taxa comprising at least 1% of total abundance are shown ranked in abundance.

Coast								
mtCOI	reads	SD	microscopy	counts	SD	18S V9	reads	SD
Temora stylifera	26.4	20.3	Undet. copepodites	37.1	6.9	Calanoida 1	13.6	17.5
Subeucalanus pileatus	24.4	30.3	Penilia spp.	13.1	8.8	Calanoida 2	10.8	12.6
Diaixis hibernica	11.9	7.0	Acartia clausi	7.4	8.5	Oikopleuridae 1	7.9	4.9
Longipedia sp.	9.2	8.6	Oncaea spp.	5.6	2.7	Calanoida 3	5.9	7.0
Centropages typicus	6.3	8.4	Appendicularia	4.5	3.3	Copepoda 1	5.8	5.7
Balanidae sp.	2.7	3.8	Paracalanus cf. parvus	4.1	3.0	Copepoda 2	5.2	0.9
Paracalanus quasimodo	2.3	1.5	Euterpina acutifrons	3.4	1.7	Eukaryota 1	4.8	4.3
Euterpina acutifrons	2.2	1.6	Clausocalanus spp.	2.3	0.5	Oikopleuridae 2	3.8	4.6
Penilia avirostris	2.1	2.9	Temora stylifera	2.2	1.4	Calanoida 4	3.3	1.6
Podon intermedius	1.4	1.6	Oithona spp.	2.2	0.9	Calanoida 5	3.3	4.6
Obelia dichotoma	1.2	1.1	Gastropoda	1.3	0.6	Calanoida 6	2.9	0.7
Acartia discaudata	1.1	2.2	Podon spp.	1.3	0.5	Eukaryota 2	2.8	0.5
Obelia sp.	1.0	2.4	Diaixis pygmaea	1.2	1.2	Eucarida 1	2.5	2.2
-			Microsetella norvegica	1.2	1.1	Siphonophorae 1	2.4	0.3
			_			Calanoida 7	2.3	0.6
						Eukaryota 3	1.6	0.2
						Oikopleuridae 3	1.5	2.0
						Aphragmophora 1	1.5	0.2
						Diplostraca 1	1.3	0.5
						Cyclopoida 1	1.1	1.3
						Sagitta sp.	1.0	0.1
Shelf				· 				
mtCOI	reads	SD	microscopy	counts	SD	18S V9	reads	SD
Subeucalanus pileatus	80.0	10.0	Undet. copepodites	43.3	7.8	Calanoida 2	20.5	1.1
Temora stylifera	9.8	6.1	Oncaea spp.	16.6	12.5	Calanoida 1	17.9	9.4
Euphausia krohni	2.1	2.5	Penilia spp.	6.1	9.9	Calanoida 8	7.1	0.7
Pleuromamma borealis	1.9	3.4	Temora stylifera	3.9	1.2	Siphonophorae 1	5.2	4.3
Clausocalanus paululus	1.3	1.6	Clausocalanus spp.	3.7	1.8	Pleuromamma abdominalis	4.4	0.4
			Paracalanus cf. parvus	3.4	2.0	Calanoida 9	4.3	0.2
			Pleuromamma spp.	2.6	1.6	Calanoida 4	4.2	1.2
			Appendicularia	1.8	3.1	Calanoida 3	3.6	0.1
			Pseudocalanus elongatus	1.8	1.2	Eucarida 1	3.5	1.0
			Lucicutia flavicornis	1.7	1.0	Oikopleuridae 2	2.2	0.0
			Evadne spp.	1.4	2.1	Diplostraca 1	2.1	2.7
			Euterpina acutifrons	1.1	0.8	Oikopleuridae 1	1.9	0.1
			Nauplius copepoda	1.1	1.1	Calanoida 7	1.6	0.6
			Oithona spp.	1.0	0.5	Aphragmophora 2	1.3	1.3
			1.1			Copepoda 2	1.1	0.7

abundances and reads was computed using the Bray-Curtis index (function <code>vegdist</code>) and then used for non-metric multidimensional scaling (NMDS). The function <code>envfit</code> was used to reveal which environmental variables correlated with the mesozooplankton community structure. The significance of sample grouping was analyzed by means of a similarity analysis (ANOSIM) which was performed with the function <code>Anosim</code>. The taxa contribution to the dissimilarity between the two groups was assessed with a SIMPER analysis. These tests were performed with the community data obtained from COI and microscopy (the low number of samples analyzed with 18S prevented these analyses).

2.6. Data archiving

Metabarcoding data (quality filtered, chimera-free merged reads) are available at Qiita repository (https://qiita.ucsd.edu/). Sequences were uploaded to GenBank, BioProject ID: PRJNA778082, BioSample accessions: SAMN22908319-31.

3. Results

3.1. Mesozooplankton taxonomic composition

According to morphological identifications (seven samples analyzed), mesozooplankton composition was dominated by the phylum Arthropoda (93.8% \pm 4.0SD of the total counts per sample, range 87.6–98.1%, Fig. 2). Within this phylum, the most abundant class was Hexanauplia (81.0 \pm 15.8%, range 57.9–97.1% of total abundance;

comprised mostly by copepods), followed by Branchiopoda (11.3 \pm 11.4%, 0.4–26.7%; composed by cladocerans). The second most abundant phylum was Chordata, represented by Appendicularia, which accounted for 3.0 \pm 3.2% (0.3–8.3%) of the total abundance. The remaining phyla comprised less than 5% of the community.

The phylum and class accounting for the largest number of reads detected by COI (13 samples analyzed; 4345 \pm 891 reads per sample after standardization) were Arthropoda (97.3 \pm 4.3% of the total reads per sample, range 84.4–99.9%, Fig. 2), and Hexanauplia (92.3 \pm 6.0% of total reads, 80.1–99.5%), respectively. Branchiopoda and Malacostraca had a similar contribution, accounting 2.4 \pm 2.9% (0.02–9.5%) and 2.6 \pm 2.7% (0–8.2%), respectively. No Appendicularia were identified by this barcode (Suppl. Table 1). The second phylum in reads number was Cnidaria, dominated by Hydrozoa, which accounted for 1.6 \pm 3.4% of the total reads abundance and up to 12.4% in sample M9. Remaining phyla reads comprised less than 5% of the community, and one taxa was not identified at phylum level by this marker (Invertebrate environmental), which represented less than 1% of the total reads assigned.

Molecular identification by 18S metabarcoding (four samples analyzed; $80,232 \pm 9446$ reads per sample after standardization) also showed that the zooplankton were mainly composed by Arthropoda, which counted for $72.5 \pm 11.5\%$ of the total reads (60.9-86.9%, Fig. 2). Hexanauplia dominated the arthropod reads ($65.3 \pm 10.6\%$, 54.0-79.2%), followed by Malacostraca ($4.3 \pm 1.7\%$, 2.5-5.8%) and Branchiopoda ($2.1 \pm 2.1\%$, 0.2-5.0%). The second group in reads number was Appendicularia ($9.9 \pm 4.6\%$, 6.1-15.3%), followed by

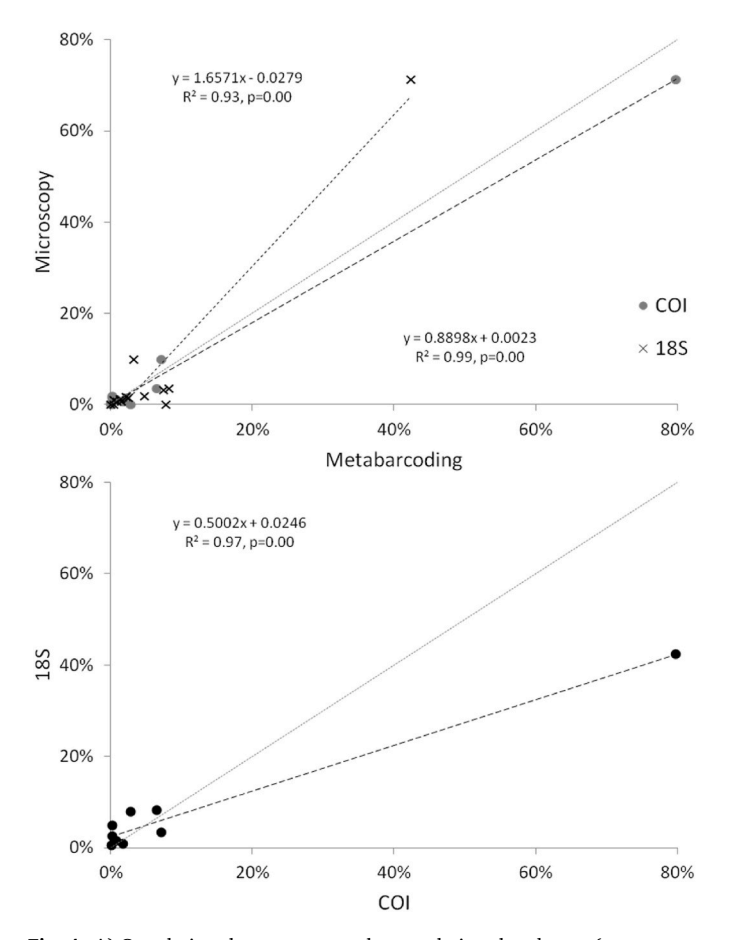


Fig. 4. A) Correlations between mean classes relative abundances (square-root transformed data) identified by microscopy and mean relative contribution of taxa to metabarcoding reads (dots: COI, crosses: 18S). B) Correlation between COI and 18S mean classes relative metabarcoding reads. Dotted line indicates 1:1 correspondence.

Hydrozoa (5.6 \pm 2.6%, 3.0–8.9%) and Chaetognatha (3.0 \pm 1.6%, 0.8–4.6%). There were seven taxa not identified at phylum level by this marker (Suppl. Table 1), representing 6.5 \pm 0.1% (1.7–14.8%) of the total reads assigned, from which 89.8% were tagged as "Eukaryota undetermined".

Copepods accounted on average for 65.3-90.7% of the total reads assigned by 18S and COI, respectively, whereas they contributed to 80.8% of the total microscope counts. Within this group, three orders were detected both by microscopy and COI metabarcoding (Calanoida, Cyclopoida and Harpacticoida), while 18S identified the orders Calanoida, Cyclopoida and Monstrilloida (Suppl. Table 1). The most abundant copepod genus according to microscopy analyses was Oncaea (27.8 \pm 20.6%, range 7.3–65.0%, Fig. 3), followed by *Temora* (10.8 \pm 7.5%, 3.0–23.7%), Acartia (9.8 \pm 15.5%, 0–44.2%) and Paracalanus (9.4 \pm 5.3%, 2.8–19.4%). However, COI reads were dominated by the largesized genus Subeucalanus (53.4 \pm 37.6%, 1.0–93.4%, Table 2), followed by Temora (20.7 \pm 18.1%, 2.6-66.5%), Diaixis (7.6 \pm 9.0%, 0–21.3%), Longipedia (6.2 \pm 10.2%, 0–32.6%) and Centropages (4.2 \pm 7.9%, 0-25.8%). These five genera accounted for 92% of the copepod COI sequences, whereas the five most abundant genera identified on the microscope gathered a 66% of the total copepod counts. Using 18S, only seven calanoid taxa were assigned to family and/or species level (Suppl. Table 1). Cladocerans contribution to relative abundances was higher when using microcopy (11.3%, 0.5-27.5% of total counts), followed by COI (4%, 0.02-9.5%) and 18S (2.1%, 0.2-5.0% of total reads). The level of identification was different depending on the approach used: order level (Diplostraca) with 18S, genus level with microscopy, and species

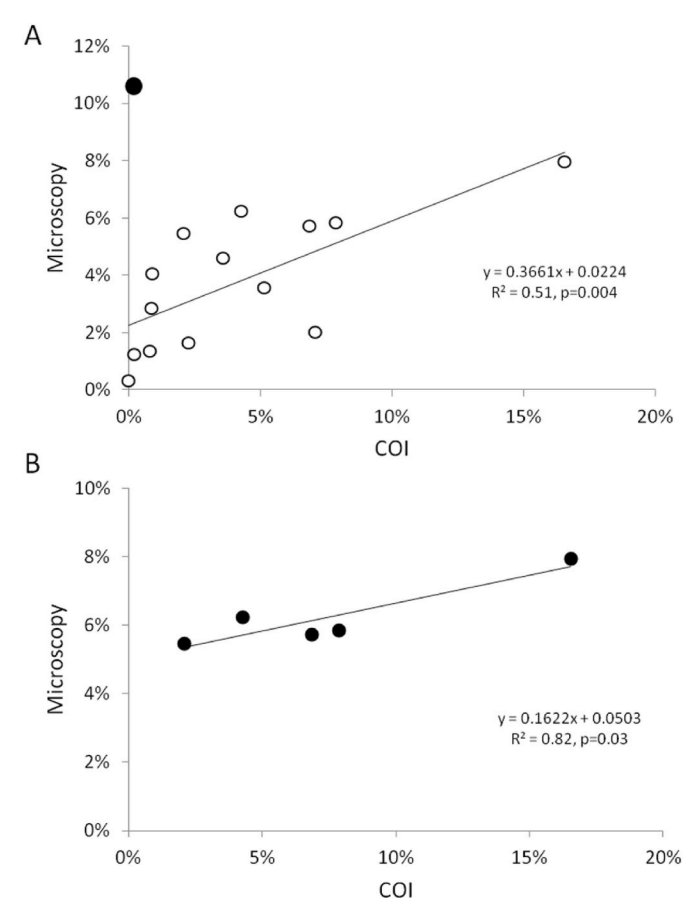


Fig. 5. Correlations between mean copepod genera relative abundances (square-root transformed data) identified by microscopy and COI metabarcoding. A) All copepod genera, except *Oncaea* (black dot, see text), B) 5 most abundant calanoid copepods (*Temora*, *Paracalanus*, *Clausocalanus*, *Acartia* and *Centropages*).

level (Evadne nordmanni, Penilia avirostris and Podon intermedius) with COI.

3.2. Comparison between methods

Total taxa number identified by microscopy (62) was lower than the number of COI OTUs (89) and 18S ASVs (754). However, standardized mean taxa richness per sample obtained from microscopic identifications (37.4 \pm 3.8) was higher than from COI metabarcoding (27.7 \pm 3.5), and both much lower than assessed from 18S (255.5 \pm 39.8). Also, mean zooplankton diversity, measured by the Shannon-Wiener index, was slightly higher when using microscopy (H' = 2.2 \pm 0.3) than when using COI (H' = 1.4 \pm 0.8); whereas H' calculated from 18S data was the highest (3.0 \pm 0.1). Copepod richness assessed by microscopy was similar to the obtained by COI (17.1 \pm 1.5 vs. 16.1 \pm 3.3), as happened with copepod diversity (H' = 1.6 \pm 0.2 vs. 1.1 \pm 0.6). However, there were no significant correlations between H' values obtained with the different methods.

We found significant positive correlations between the mean class level relative abundances (square-root transformed data) estimated from microscopic counts and the mean relative contribution of taxa to metabarcoding reads of the two molecular markers (COI: $r^2 = 0.99$, p = 0.00; 18S: $r^2 = 0.93$, p = 0.00, Fig. 4a). We also observed a significant correlation between relative reads from both molecular markers ($r^2 = 0.97$, p = 0.00, Fig. 4b).

Within Copepoda, we detected 24 genera through microscopy and 22 genera by COI metabarcoding, of which 15 were identified by both

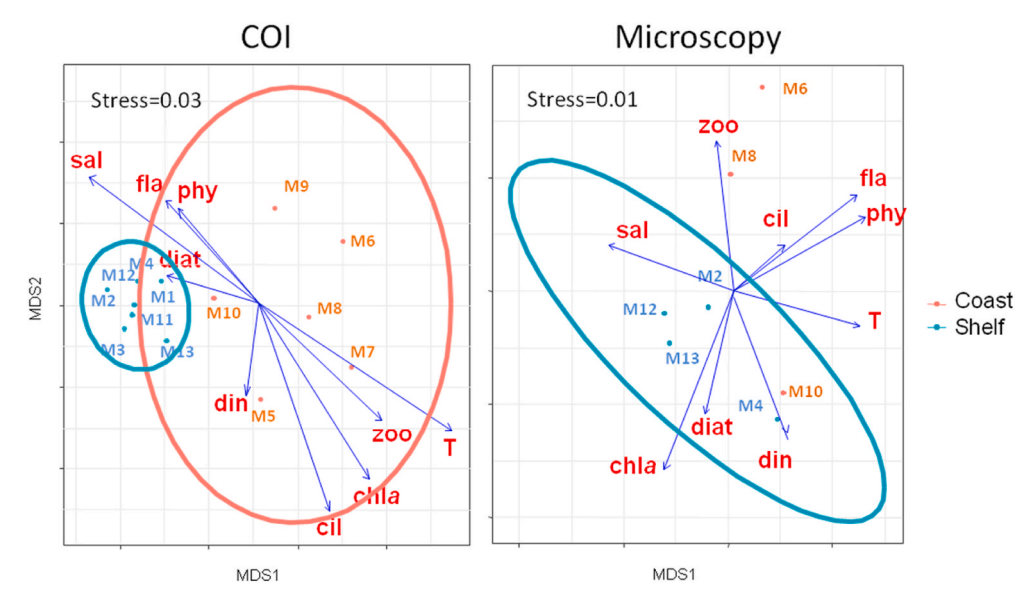


Fig. 6. Community structure NMDS defined by COI (13 samples) and by microscopy data (7 samples).

techniques (Suppl. Table 1). Further, six genera were not detected through microscopy but were in the COI samples, meanwhile nine genera were not detected by COI metabarcoding and were present in the morphological samples (Suppl. Table 1). We observed a positive and significant correlation between the copepod genera mean relative abundances (square-root transformed data) obtained by microscopy and COI, after excluding the small copepod Oncaea (Fig. 5a), which dominated microscopic counts (10.8%) but was barely detected by COI (0.2%). We also found a positive and significant correlation between mean microscopic counts (considered as relative abundances) and COI reads (after standardization) for the most abundant calanoid copepod genera according to morphological identifications (i.e. Temora, Paracalanus, Clausocalanus, Acartia and Centropages, Fig. 5b). Significant positive correlations between the relative contribution of counts and reads (square-root transformed data) at each station were also found for the genera Acartia, Ctenocalanus, Euterpina, and Pleuromamma (Suppl. Fig. 1).

At the species level, 31 copepod taxa were identified by microscopy and 37 by COI barcoding, with 15 genera and 10 species in common. Calanus helgolandicus, identified under the microscope, was wrongly assigned to C. euxinus by COI. The sequence variation observed between these species is known to be lower than their intraspecific variability (e. g., <0.5% for COI, Unal et al., 2006; <0.4% for mt16S, Yebra et al., 2011). As C. euxinus is absent in the Mediterranean Sea (Yebra et al., 2011; Razouls et al., 2021), we renamed it as identified by morphology, prior to the comparison between methods. We observed positive correlations between relative abundances (square-root data) for Acartia clausi, A. discaudata, Ctenocalanus vanus and Euterpina acutifrons (Suppl. Fig. 1). Through 18S we identified seven copepod species, with one in common with microscopic identifications (Isias clavipes) and two in common with COI results (Pleuromamma abdominalis and Subeucalanus pileatus). Within Cladocera, correlations between relative COI sequence reads and abundance counts were not significant. No comparison was possible with 18S results, as only one ASV was assigned to specific enough level (Penilia avirostris).

Combining microscopy and metabarcoding, a total of 58 copepod species were identified in this study, 34 were detected first time within the Bay of Malaga and 15 of them were new records for the Alboran Sea (Suppl. Table 2). The known copepods biodiversity in the North Alboran Sea thus increased in a 9.3%, up to a total of 161 species.

3.3. Spatio-temporal community pattern

Ordination of the 13 samples based on COI reads grouped them in two clusters, matching sampling time and their distance to the coast/ bottom depth: coast-night (stations 5 to 10, avg. bottom depth 21 m) and shelf-day (sts. 1-4, 11-13, avg. depth 47-72 m) (Fig. 6, Table 1). The statistical significance of the grouping was assessed with the ANOSIM test (R = 0.90, p = 0.002). It is notable that the coast samples that were collected during the same night at 2 h intervals were scattered in the ordination plot compared to the shelf ones that were tightly grouped, despite being sampled during two consecutive days (light hours) over a broader bottom depth range, indicating a lower variability in the shelf community structure than in shallow waters. Among the seven samples analyzed with the microscope, the ordination plot also discriminated the shelf samples from those obtained in the coast, however the grouping was not statistically significant (ANOSIM, R = 0.31, p = 0.11), probably due to the low amount of analyzed samples. For the same data set (n = 7), discrimination between shelf and coast was also obtained for COI, although this time the differences between the two groups were statistically significant (ANOSIM, R = 0.72, p = 0.04, Suppl. Fig. 2).

There were not clear relationships between the environmental variables and the community structure based on COI, apart from temperature ($r^2 = 0.49$, p = 0.03). However, chlorophyll a showed a positive correlation with the structure of the mesozooplankton community obtained with microscopy ($r^2 = 0.77$, p = 0.04).

Low sample size prevented performing ANOSIM on the 18S dataset, although some differences between coast and shelf zones at the phylum level were also observed (n = 4, Fig. 7). Arthropoda mean contribution to 18S reads increased a 16.1% from the coast to the shelf, while Eukaryota decreased by 9%, Cnidaria 2.7%, and Chordata and Mollusca 1% each. Mean contribution of Arthropoda and Radiozoa assessed through microscopy decreased by 3.8% and 1.2%, respectively, from the coast to the shelf. This was coupled with an increase in the mean percentage of Chordata (2%) and Mollusca (1.7%) in the shelf. However, the mean relative phyla abundances of COI reads remained similar in both zones, only a slight decrease in relative abundances of Cnidaria (1.3%) from the coast to the shelf was observed.

The main contributors to the differences observed between zones by COI were copepods (*Subeucalanus pileatus, Diaixis hibernica, Longipedia* sp., *Temora stylifera and Centropages typicus*, Table 2, Fig. 8); whereas differences in the samples analyzed by microscopy were driven by a combination of copepods (*Oncaea* spp., undetermined copepodites,

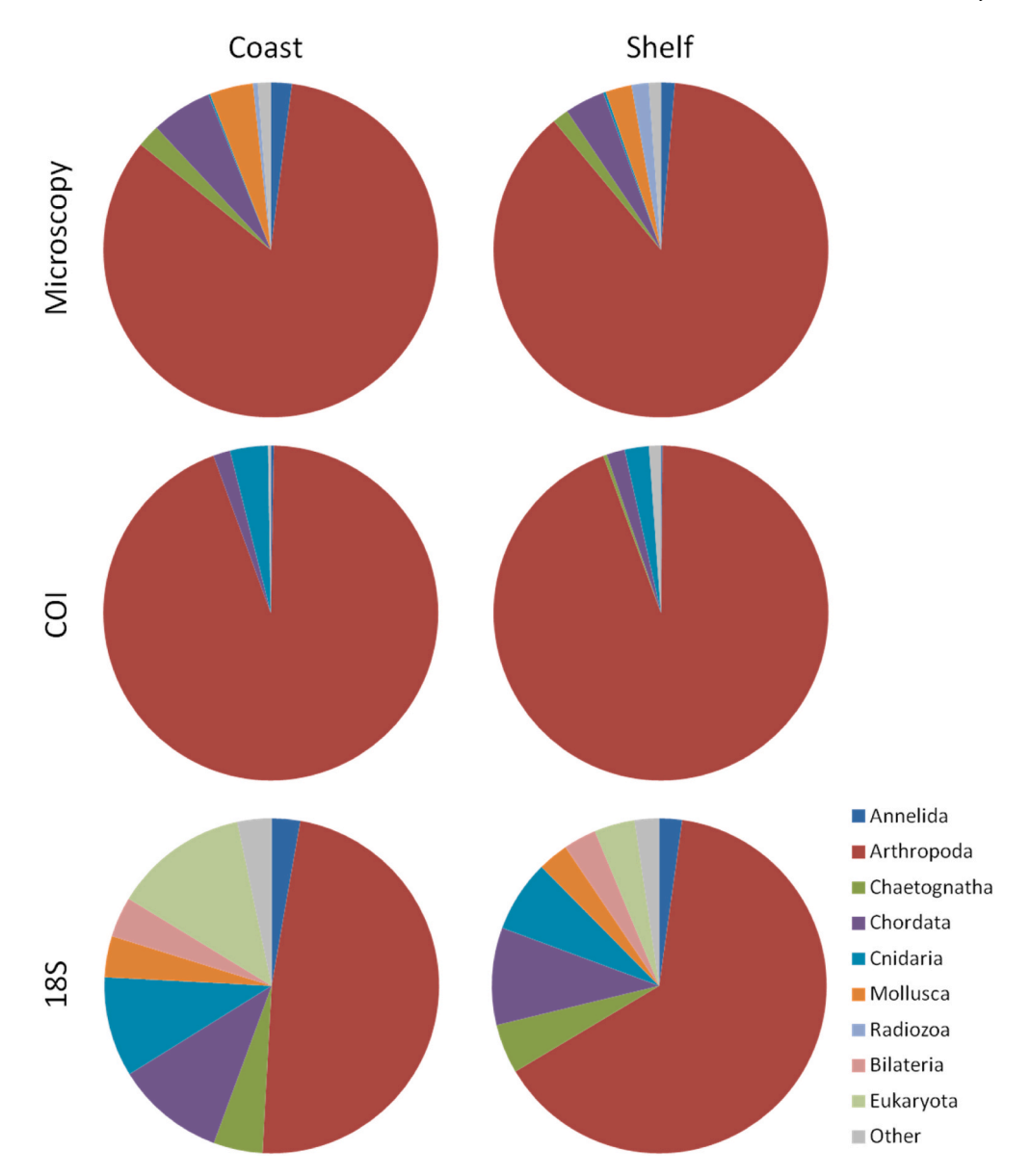


Fig. 7. Field mesozooplankton relative phyla abundances identified by A) microscopy, B) COI, and C) 18S, averaged for each zone. Taxa with abundance <1%, or not identified to phylum level, were grouped in Other.

Acartia clausi), the cladocera Penilia sp., and Appendicularia, as revealed by the SIMPER analyses (Suppl. Table 3).

4. Discussion

Two distinct mesozooplankton communities were observed within the Bay of Malaga, corresponding to coastal and shelf waters. The shelf community was dominated by copepods (73–96% of the total abundance), whereas the coastal waters presented a more diverse community in which the non-copepod taxa (mainly cladocerans and appendicularians) represented 12–42% of the total abundances. This spatial structuring, detected both by microscopy and metabarcoding, is in agreement with the zonation recently described for zooplankton communities derived from backscatter data (Ventero et al., 2020) and time series morphological analyses (Yebra et al., 2022). Our high frequency sampling further revealed that the coastal community presented higher variability in species composition during the night than the shelf during light hours, despite the reduced bottom depth range in the shallow waters. Unexpectedly, the relationship between the communities' structure and the environmental variables was limited: the community

variability depicted based on COI was only related to temperature, and the microscopy-based community correlated to chlorophyll. Thus, other factors that were not monitored during our study such as predation pressure might be driving the short-term variability in the structure of the mesozooplankton communities. In this sense, small pelagic zooplanktivorous fish larvae undergo diel migrations inshore-offshore in the study area, schooling in shallow waters at night (presumably to avoid predation) and dispersing in the shelf water column by day to prey on zooplankton (Yebra et al., 2019). The latter study also showed that sardine larvae do not feed at night; nonetheless, the concentration of predators in shallow waters might affect the zooplankton assemblages, as it has been found that the presence of fish chemical cues affects the behavior and fitness of copepods (Kvile et al., 2021). Further studies would be needed to understand the drivers of such short-term variability within the coastal mesozooplankton communities in the region.

The three approaches used to study the composition of the samples (microscopy, COI and 18S) led to significantly similar results at phylum and class taxonomic levels. Comparative studies so far have been made on the large spatial and or temporal scale, e.g. time series (Abad et al., 2017; Stern et al., 2018; Bucklin et al., 2019), whereas in this work we

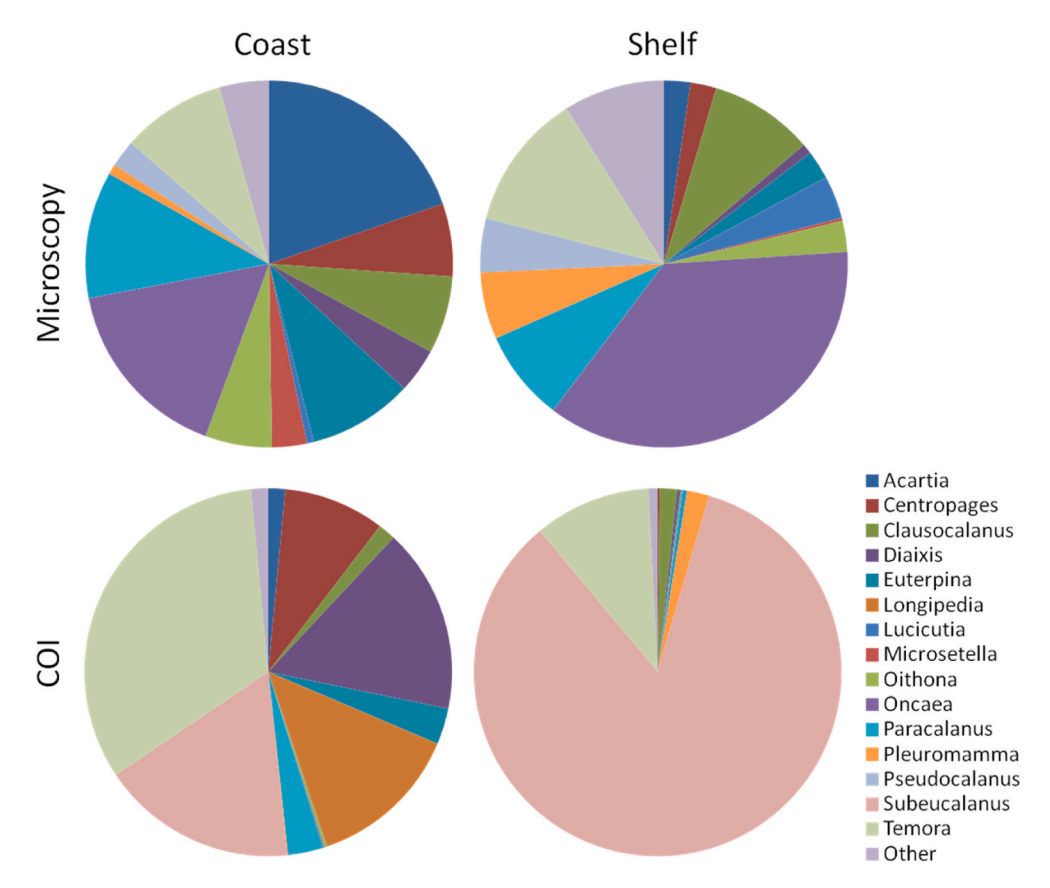


Fig. 8. Field copepod relative genera abundances identified by A) microscopy and B) COI, averaged for each zone. Taxa with abundance <1% were grouped in Other.

strived to see how metabarcoding performed to detect short time and space scale heterogeneity in the zooplankton communities. Given that the mesozooplankton community in the study area was composed by up to 98% arthropods and that they were effectively identified by COI, this marker seems a suitable tool to be used for mesozooplankton biodiversity studies in the region. This was further supported by the significant relationship found between microscopic counts and COI reads of the most abundant calanoid copepods. However, looking at the taxa responsible for the dissimilarities between communities we found discrepancies between microscopy counts and COI reads. The shelf waters by day were dominated by copepods: the calanoid Subeaucalanus pileatus accounted for 60% of COI reads, but the cyclopoid Oncaea spp. and undertermined copepodites represented half of the microscopy counts. This mismatch might be related to the high percentage of copepodites not identified under the microscope, but also most likely to the differences in biomass between the dominant species. Large individual biomass (implying high amount of genes copies per individual) of Eucalanidae could lead to the higher relative contribution to the total COI reads, coupled with lower than expected assignment to the small copepods such as Oithona and Oncaea, which represented 6-19% of microscopic counts but were only weakly detected by COI metabarcoding at some stations (<1% of reads). Many other small and relatively rare genera were not detected by metabarcoding either, such as Microsetella or Corycaeus (<5% of copepod relative abundance). Furthermore, the COI reads in the shallow coastal waters were dominated at night by other calanoid copepods such as Temora stylifera and Diaixis hibernica; whereas microscopic counts were dominated by the cladocera Penilia, the cyclopoid Oncaea and copepodites. Thus, the taxa driving the differentiation between coastal and shelf communities were different depending on the method used. According to morphological analyses, the five main contributors to the dissimilarities between communities included copepods, cladocerans and appendicularians; whereas the main drivers of the differences between groups depicted by

COI were copepods. This may be due to the absence of Appendicularia reads in the COI samples, despite they were detected by both microscopy and 18S metabarcoding. Given that Appendicularians represent the most abundant group after crustaceans in the region (Mercado et al., 2007; Yebra et al., 2022), COI might not be an adequate stand-alone marker and a combination with other such as 18S or ITS (Garić et al., 2018) would be needed to successfully implement metabarcoding as the sole tool for studying the zooplankton communities.

The low sample size and lower taxonomic resolution of the 18S prevented a comparison between communities at the same level as the described by microscopy and COI. Nevertheless, 18S detected several large taxa (Chordata, Mollusca, Echinodermata, Ctenophora) that were not efficiently amplified by COI nor identified to family level under the microscope. 18S might be then a suitable complementary marker for COI, as COI did not amplify important groups such as Appendicularians, Thaliacea, Echinoderms and Radiozoa. On the other hand, 18S lacks the specificity required for species richness or diversity studies, as only a few taxa were identified to the species level, meanwhile most assignments were shared by taxa from the same family or above. This lack of specificity provides less information at species level than previous studies based on microscopy. For meta-community ecology studies, where species level identity is not essential, a marker such as 18S, with lower resolution but able to amplify most of the community, may give a better answer than COI. However, if detailed taxonomy of the community is needed, such in biodiversity studies, then a combination of microscopy and COI would be the best option, although with a thorough prescreening on primer amplification limits. In our study, such combination of methods facilitated the identification at species level of cryptic copepod species, such as Paracalanus (Kasapidis et al., 2018), significantly increasing the list of copepod species and highlighting the as yet hidden diversity in SW Mediterranean waters.

The study area is a complex hydrodynamic region, which is one of the areas with the highest plankton productivity and biodiversity of the Mediterranean Sea. The three methods applied detected the heterogeneity within the high-frequency short-term study, however they performed differently. Metabarcoding of COI and 18S provided fast costeffective results, although 18S is lacking the specific resolution required for biodiversity studies, and is COI failing to detect major groups with increasing importance in the region (e.g. appendicularians and doliolids, Yebra et al., 2022). Also, given the current mismatch between relative abundances obtained by reads and counts for some taxa, and to keep continuity with previous studies, the assessment of the community composition by microscopy cannot be substituted by metabarcoding in the region. The statistical comparison of spatio-temporal mesozooplankton variability conducted based on morphological and molecular analyses is an important step toward the assessment of metabarcoding suitability in marine zooplankton biodiversity studies, and further comparisons between microscopic counts and COI reads are needed to validate and strengthen the correlations observed between relative abundances of key species obtained by both methods. Based in our results, we propose the development of an integrative approach which would couple the morphological identification of major groups, which has been recently optimized in our waters to reduce processing time through semi-automated image analysis (Valcarcel-Pérez et al., 2019), with a molecular assignation of copepod species, the dominant mesozooplankton group. Then, species relative reads abundance within each genus may be used to infer the relative copepod species density within each sample, incorporating results obtained by both approaches into a single integrated result. We are aware that nowadays this integrative approach is not a straight forward process (Laakmann et al., 2020) and expert taxonomists are very much needed to validate results obtained by these new techniques. Nonetheless, the increasing advances in image analyses-machine learning (Picheral et al., 2017; Orenstein et al., 2022) as well as the ongoing international efforts to populate curated DNA databases (Bucklin et al., 2021), would allow in the near future the production and integration of large combined datasets, facilitating the assessment and monitoring of mesozooplankton biodiversity and the response of coastal communities to the global change.

CRediT authorship contribution statement

Lidia Yebra: Writing – review & editing, Writing – original draft, Visualization, Investigation, Funding acquisition, Formal analysis, Conceptualization. Candela García-Gómez: Writing – review & editing, Investigation, Formal analysis. Nerea Valcárcel-Pérez: Writing – review & editing, Visualization, Investigation, Formal analysis. Alma Hernández de Rojas: Writing – review & editing, Investigation, Formal analysis. Leocadio Blanco-Bercial: Writing – review & editing, Formal analysis, Data curation. M. Carmen Castro: Writing – review & editing, Investigation. Francisco Gómez-Jakobsen: Writing – review & editing, Visualization. Jesús M. Mercado: Writing – review & editing, Formal analysis.

Declaration of competing interest

The authors declare that they have no known competing financial interests or personal relationships that could have appeared to influence the work reported in this paper.

Data availability

Links to data not included in the article are provided within the text.

Acknowledgements

We thank the crew and colleagues on board RV Francisco de Paula Navarro for their help during sampling. We are indebted to Naiara Rodríguez-Ezpeleta (AZTI, Sukarrieta, Spain) for kindly sharing the unpublished sequence of a fish blocking primer, and ICES WGIMT members for stimulating discussions. We also thank the technical and human support of SGIker (UPV/EHU, MICINN, GV/EJ, ESF) and Unidad de Genómica Fundación Parque Científico de Madrid (FPCM/UAM). This work was funded by the Consejería de Economía, Innovación y Ciencia of the Andalusian Government through project MOLDIALB (P11-RMN-7354) and partially supported by project MICROZOO-ID (P20_00743). C.G.C. and N.V.P. were supported by contracts within the Program Personal Técnico de Apoyo funded by the Spanish Ministry of Economy, Industry and Competitiveness. L.B.B. was partially supported by the US National Science Foundation under Grant OCE-1948162.

Appendix A. Supplementary data

Supplementary data to this article can be found online at https://doi.org/10.1016/j.ecss.2022.108038.

References

- Abad, D., Albaina, A., Aguirre, M., Estonba, A., 2017. 18S V9 metabarcoding correctly depicts plankton estuarine community drivers. Mar. Ecol. Prog. Ser. 584, 31–43.
- Albaina, A., Aguirre, M., Abad, D., Santos, M., Estonba, A., 2016. 18S rRNA V9 metabarcoding for diet characterization: a critical evaluation with two sympatric zooplanktivorous fish species. Ecol. Evol. 6, 1809–1824.
- Altschul, S.F., Gish, W., Miller, W., Myers, E.W., Lipman, D.J., 1990. Basic local alignment search tool. J. Mol. Biol. 215, 403–410.
- Amaral-Zettler, L.A., McCliment, E.A., Ducklow, H.W., Huse, S.M., 2009. A method for studying protistan diversity using massively parallel sequencing of V9 hypervariable regions of small-subunit ribosomal RNA genes. PLoS One 4, e6372.
- Bedford, J., Ostle, C., Johns, D.G., Atkinson, A., Best, M., Bresnan, E., Machairopoulou, M., et al., 2020. Lifeform indicators reveal large-scale shifts in plankton across the North-West European shelf. J. Global Change Biol. 26-6, 3482-3407
- Blanco-Bercial, L., 2020. Metabarcoding analyses and seasonality of the zooplankton community at BATS. Front. Mar. Sci. 7.
- Bucklin, A., Lindeque, P.K., Rodriguez-Ezpeleta, N., Albaina, A., Lehtiniemi, M., 2016. Metabarcoding of marine zooplankton: prospects, progress and pitfalls. J. Plankton Res. 38, 393–400. https://doi.org/10.1093/plankt/fbw023.
- Bucklin, A., Yeh, H.D., Questel, J.M., Richardson, D.E., Reese, B., Copley, N.J., Wiebe, P. H., 2019. Time-series metabarcoding analysis of zooplankton diversity of the NW Atlantic continental shelf. ICES (Int. Counc. Explor. Sea) J. Mar. Sci. 76, 1162–1176. https://doi.org/10.1093/icesjms/fsz021.
- Bucklin, A., Peijnenburg, K.T.C.A., Kosobokova, K.N., O'Brien, T.D., Blanco-Bercial, L., Cornils, A., Falkenhaug, T., et al., 2021. Toward a global reference database of COI barcodes for marine zooplankton. Mar. Biol. 168, 78. https://doi.org/10.1007/ s00227-021-03887-v.
- Clarke, K.R., Gorley, R.N., 2015. PRIMER V7: User Manual/Tutorial. PRIMER-E, Plymouth, p. 296.
- Coll, M., Piroddi, C., Steenbeek, J., Kaschner, K., Ben Rais Lasram, F., Aguzzi, J., Ballesteros, E., et al., 2010. The biodiversity of the Mediterranean Sea: estimates, patterns, and threats. PLoS One 5 (8), e11842. https://doi.org/10.1371/journal. pone.0011842.
- Corell, J., Rodríguez-Ezpeleta, N., 2014. Tuning of protocols and marker selection to evaluate the diversity of zooplankton using metabarcoding. Revista de Investigación Marina, AZTI-Tecnalia 21 (2), 19–39. www.azti.es/RIM.
- Cornils, A., Held, C., 2014. Evidence of cryptic and pseudocryptic speciation in the *Paracalanus parvus* species complex (Crustacea, Copepoda, Calanoida). Front. Zool.
- Edgar, R.C., 2016. UNOISE2: improved error-correction for Illumina 16S and ITS amplicon sequencing. bioRxiv, 081257.
- Edgar, R.C., Haas, B.J., Clemente, J.C., Quince, C., Knight, R., 2011. UCHIME improves sensitivity and speed of chimera detection. Bioinformatics 27, 2194–2200.
- García, A., Pérez de Rubín, J., Rodríguez, J.M., 1988. La distribución de las áreas de puesta de la sardina (Sardina pilchardus Walb.) en el sector noroccidental costero del Mar de Alborán en marzo de 1982, vol. 56. Informes Técnicos del Instituto Español de Oceanografía, pp. 1–24.
- García-Gómez, C., Yebra, L., Cortés, D., Sánchez, A., Alonso, A., Valcárcel-Pérez, N., Gómez-Jakobsen, F., et al., 2020. Metabarcoding unveils shifts in the protist community diversity associated to environmental gradients. FEMS (Fed. Eur. Microbiol. Soc.) Microbiol. Ecol. 96, fiaa197. https://doi.org/10.1093/femsec/ fiaa197.
- Garić, R., Pfannkuchen, M., Dénes, M., Gissi, C., Flood, P.R., Batistić, M., 2018. Challenges in Appendicularian Integrative Taxonomy and Barcoding. ICES Annual Science Conference, Hamburg.
- Giannoulaki, M., Iglesias, M., Tugores, M.P., Bonnano, A., Patti, B., De Felice, A., Leonori, I., et al., 2013. Characterizing the potential habitat of European anchovy Engraulis encrasicolus in the Mediterranean Sea, at different life stages. Fish. Oceanogr. 22, 69–89. https://doi.org/10.1111/fog.12005.
- Gómez-Jakobsen, F.J., Mercado, J.M., Cortés, D., Yebra, L., Salles, S., 2019. A first description of the summer upwelling off the Bay of Algeciras and its role in the

- northwestern Alboran Sea. Estuar. Coast Shelf Sci. 225, 106230 https://doi.org/10.1016/j.ecss.2019.05.012.
- Hirai, J., Katakura, S., Kasai, H., Nagai, S., 2017. Cryptic zooplankton diversity revealed by a metagenetic approach to monitoring metazoan communities in the coastal waters of the Okhotsk Sea, Northeastern Hokkaido. Front. Mar. Sci. 4, 379. https://doi.org/10.3389/fmars.2017.00379.
- Kasapidis, P., Siokou, I., Khelifi-Touhami, M., Mazzocchi, M.G., Matthaiaki, M., Christou, E., Fernandez de Puelles, M.L., et al., 2018. Revising the taxonomic status and distribution of the *Paracalanus parvus* species complex (Copepoda, Calanoida) in the Mediterranean and Black Seas through an integrated analysis of morphology and molecular taxonomy. J. Plankton Res. 40, 595–605. https://doi.org/10.1093/ plankt/fbv036.
- Kvile, K.Ä., Altin, D., Thommesen, L., Titelman, J., 2021. Predation risk alters life history strategies in an oceanic copepod. Ecology 102 (1), e03214. https://doi.org/ 10.1002/ecv.3214.
- Laakmann, S., Blanco-Bercial, L., Cornils, A., 2020. The crossover from microscopy to genes in marine diversity – from species to assemblages in marine pelagic copepods. Phil. Trans. R. Soc. B 375, 20190446. https://doi.org/10.1098/rstb.2019.0446.
- Leray, M., Yang, J.Y., Meyer, C.P., Mils, S.C., Agudelo, N., Ranwez, V., Boehm, J.T., Machida, R.J., 2013. A new versatile primer set targeting a short fragment of the mitochondrial COI region for metabarcoding metazoan diversity: application for characterizing coral reef fish gut contents. Front. Zool. 10, 34. https://doi.org/10.1186/1742-9994-10-34
- Lindeque, P.K., Parry, H.E., Harmer, R.A., Somerfield, P.J., Atkinson, A., Ianora, A., 2013. Next generation sequencing reveals the hidden diversity of zooplankton assemblages. PLoS One 8, e81327. https://doi.org/10.1371/journal.pone.0081327.
- Mercado, J.M., Cortés, D., García, A., Ramírez, T., 2007. Seasonal and inter-annual changes in the planktonic communities of the northwest Alboran Sea (Mediterranean Sea). Prog. Oceanogr. 74 (2–3), 273–293. https://doi.org/10.1016/j. pocean.2007.04.013.
- Meyer, C., 2003. Molecular systematics of cowries (Gastropoda: Cypraeidae) and diversification patterns in the tropics. Biol. J. Linn. Soc. 79, 401–459. https://doi. org/10.1046/j.1095-8312.2003.00197.x.
- Micheli, F., Halpern, B.S., Walbridge, S., Ciriaco, S., Ferretti, F., Fraschetti, S., Lewison, R., et al., 2013. Cumulative human impacts on Mediterranean and black Sea marine ecosystems: assessing current pressures and opportunities. PLoS One 8 (12), e79889. https://doi.org/10.1371/journal.pone.0079889.
- Oksanen, J., Blanchet, F.G., Friendly, M., Kindt, R., Legendre, P., McGlinn, D., Minchin, P.R., et al., 2019. Vegan: community ecology package. URL. https://cran.r-project.org. https://github.com/vegandevs/vegan. version 2.5-6, 1–296.
- Orenstein, E., Ayata, S.D., Maps, F., Biard, T., Becker, E., Benedetti, F., de Garidel-Thoron, T., et al., 2022. Machine learning techniques to characterize functional traits of plankton from image data. Limnol. Oceanogr. https://doi.org/10.1002/lpo.12101.
- Picheral, M., Colin, S., Irisson, J.-O., 2017. EcoTaxa, a tool for the taxonomic classification of images. http://ecotaxa.obs-vlfr.fr/.
- Quast, C., Pruesse, E., Yilmaz, P., Gerken, J., Schweer, T., Yarza, P., Peplies, J., et al., 2013. The SILVA ribosomal RNA gene database project: improved data processing and web-based tools. Nucleic Acids Res. 41, D590-D596
- and web-based tools. Nucleic Acids Res. 41, D590–D596.

 Questel, J.M., Hopcroft, R.R., DeHart, H.M., Smoot, C.A., Kosobokova, K.N., Bucklin, A., 2021. Metabarcoding of zooplankton diversity within the Chukchi Borderland, Arctic Ocean: improved resolution from multi-gene markers and region-specific DNA databases. Mar. Biodivers. 51. 4.
- Razouls, C., Desreumaux, N., Kouwenberg, J., de Bovée, F., 2021. Biodiversity of Marine Planktonic Copepods (Morphology, Geographical Distribution and Biological Data). Sorbonne University, CNRS. Available at. http://copepodes.obs-banyuls.fr/en. (Accessed 23 February 2021). Accessed.
- Richardson, A.J., 2008. In hot water: zooplankton and climate change. ICES (Int. Counc. Explor. Sea) J. Mar. Sci. 65, 279–295. https://doi.org/10.1093/icesjms/fsn028. Rose, M., 1933. Copépodes pélagiques. Faune Fr. 26, 1–374.

- Sarhan, T., García-Lafuente, J., Vargas, M., Vargas, J.M., Plaza, F., 2000. Upwelling mechanisms in the northwestern Alboran Sea. J. Mar. Syst. 23, 317–331.
- Schloss, P.D., Westcott, S.L., Ryabin, T., Hall, J.R., Hartmann, M., Hollister, E.B., Lesniewski, R.A., et al., 2009. Introducing mothur: open-source, platformindependent, community-supported software for describing and comparing microbial communities. Appl. Environ. Microbiol. 75, 7537–7541.
- Schroeder, A., Pallavicini, A., Edomi, P., Pansera, M., Camatti, E., 2021. Suitability of a dual COI marker for marine zooplankton DNA metabarcoding. Mar. Environ. Res. 170, 105444.
- Stefanni, S., Stanković, D., Borme, D., de Olazabal, A., Juretić, T., Pallavicini, A., Tirelli, V., 2018. Multi-marker metabarcoding approach to study mesozooplankton at basin scale. Sci. Rep. 8, 12085 https://doi.org/10.1038/s41598-018-30157-7.
- Steinberg, D.K., Landry, M.R., 2017. Zooplankton and the ocean carbon cycle. Ann. Rev. Mar. Sci 9, 413–444. https://doi.org/10.1146/annurev-marine-010814-015924.
- Stern, R., Kraberg, A., Bresnan, E., Kooistra, W.H.C.F., Lovejoy, C., Montresor, M., Moran, X.A.G., et al., 2018. Molecular analyses of protists in long-term observation programmes-current status and future perspectives. J. Plankton Res. 40 (5), 519–536. https://doi.org/10.1093/plankt/fby035.
- Trégouboff, G., Rose, M., 1957. Manuel de Planctonologie méditerranéenne. Edit. Centre National de la Recherche Scientifique, Paris, Tome I, pp. 1–587. ; Tome II (Planches): I-XXXIX + Tableau de diagnose des familles et des genres (Copépodes).
- Unal, E., Frost, B.W., Armbrust, V., Kideys, A.E., 2006. Phylogeography of Calanus helgolandicus and the black Sea copepod Calanus euxinus, with notes on Pseudocalanus elongatus (Copepoda, Calanoida). Deep-Sea Res. Part II Top. Stud. Oceanogr. 53 (17–19), 1961. https://doi.org/10.1016/J.DSR2.2006.03.017, 1975.
- Utermöhl, H., 1958. Zur Ver vollkommung der quantitative phytoplankton-methodik. Mitteilung Internationale Vereinigung Fuer Theoretische unde Amgewandte. Limnologie 9, 39.
- Valcárcel-Pérez, N., Yebra, L., Herrera, I., Mercado, J., Gómez-Jakobsen, F., Salles, S., 2019. Usefulness of semiautomatic image analysis for the assessment of zooplankton community structure in a highly dynamic area of the Alboran Sea (SW Mediterranean). Book of Abstracts II International Congress of Young Marine Researchers. CEIMAR, 10/2019. ISBN 978-84-09-13664-3.
- Ventero, A., Iglesias, M., Miquel, J., 2020. From coast to slope: zooplankton communities shift in the Northern Alboran Sea, estuarine. Coast. Shelf Sci. 242, 106854 https:// doi.org/10.1016/j.ecss.2020.106854.
- Yebra, L., Bonnet, D., Harris, R.P., Lindeque, P., Peijnenburg, K., 2011. Barriers in the pelagic: population structuring of *Calanus helgolandicus* and *C. euxinus* in European waters. Mar. Ecol. Prog. Ser. 428, 135–149. https://doi.org/10.3354/meps09056.
- Yebra, L., Espejo, E., Putzeys, S., Giráldez, A., Gómez-Jakobsen, F., León, P., Salles, S., et al., 2020. Zooplankton biomass depletion event reveals the importance of small pelagic fish top-down control in the Western Mediterranean coastal waters. Front. Mar. Sci. 7, 608690 https://doi.org/10.3389/fmars.2020.608690.
- Yebra, L., Hernández de Rojas, A., Valcárcel-Pérez, N., Castro, M.C., García-Gómez, C., Cortés, D., Mercado, J.M., et al., 2019. Molecular identification of the diet of Sardina pilchardus larvae in the SW Mediterranean Sea. Mar. Ecol. Prog. Ser. 617-618, 41–52. https://doi.org/10.3354/meps12833.
- Yebra, L., Herrera, I., Mercado, J.M., Cortés, D., Gómez-Jakobsen, F., Alonso, A., Valcárcel-Pérez, N., et al., 2018. Zooplankton production and carbon export flux in the western Alboran Sea gyre (SW Mediterranean). Prog. Oceanogr. 167, 64–77. https://doi.org/10.1016/j.pocean.2018.07.009.
 Yebra, L., Putzeys, S., Cortés, D., Mercado, J.M., Gómez-Jakobsen, F., León, P.,
- Yebra, L., Putzeys, S., Cortes, D., Mercado, J.M., Gomez-Jakobsen, F., Leon, P., Herrera, I., et al., 2017. Trophic conditions govern summer zooplankton production variability along the SE Spanish coast (SW Mediterranean). Estuarine. Coast. Shelf Sci. 187, 134–145. https://doi.org/10.1016/j.ecss.2016.12.024.
- Yebra, L., Puerto, M., Valcárcel-Pérez, N., Putzeys, S., Gómez-Jakobsen, F., García-Gómez, C., Mercado, J.M., 2022. Spatio-temporal variability of the zooplankton community structure in the SW Mediterranean 1992-2020: linkages with environmental drivers. Prog. Oceanogr. 203, 102782 https://doi.org/10.1016/j.pocean.2022.102782.